Zeolite Synthesis Using Hierarchical Structure-Directing Surfactants: Retaining Porous Structure of Initial Synthesis Gel and Precursors

DATASET *in* CHEMISTRY OF MATERIALS · JULY 2012

Impact Factor: 8.35 · DOI: 10.1021/cm300841v

5 AUTHORS, INCLUDING:

Kanghee Cho
Institute for Basic Science
16 PUBLICATIONS **574** CITATIONS
SEE PROFILE

Kyungsu Na
Korea Advanced Institute of Science and Tech…
16 PUBLICATIONS **1,401** CITATIONS
SEE PROFILE

Osamu Terasaki
Stockholm University
453 PUBLICATIONS **21,375** CITATIONS
SEE PROFILE

CHEMISTRY OF MATERIALS

Article

pubs.acs.org/cm

Zeolite Synthesis Using Hierarchical Structure-Directing Surfactants: Retaining Porous Structure of Initial Synthesis Gel and Precursors

Kanghee Cho,[†,‡] Kyungsu Na,[†,‡] Jaeheon Kim,[†] Osamu Terasaki,[§] and Ryong Ryoo*[,†,‡]

[†]Center for Functional Nanomaterials, Department of Chemistry, [‡]Graduate School of Nanoscience and Technology (WCU), and [§]Graduate School of EEWS (WCU), KAIST, Daejeon 305-701, Korea

ABSTRACT: Zeolite beta with a mesopore-micropore hierarchy is hydrothermally synthesized here using various surfactants that can function as a hierarchical structure-directing agent at both the meso- and microstructural levels. Tetraethoxysilane and diatomaceous earth were tested as the silica sources. The pore size distribution of the zeolite was analyzed by N_2 adsorption and electron microscopy. The result was related to the surfactant structure, silica source, and Na^+ concentration. The zeolite showed quite uniform mesopores corresponding to the surfactant micelles, in addition to zeolitic micropores generated by the surfactant head groups. Furthermore, an additional level of large pores (≥20 nm) could be obtained as a result of the retaining of pores from the initial synthesis gel or the zeolite precursor. The large pores were fully retained when the silica source was transformed into a crystalline zeolite via pseudomorphic transformation without migration into the solution phase. The transformation could be controlled by the choice of the synthesis conditions and surfactants. The resultant zeolite with a macropore-mesopore-micropore hierarchy shows potential applicability where facile diffusion is required.

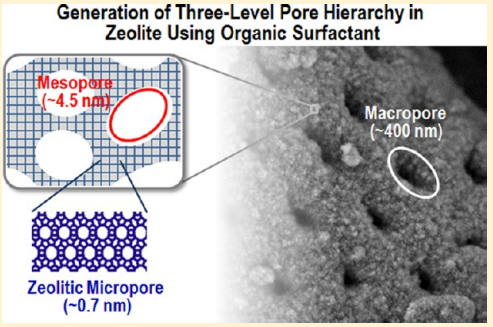

KEYWORDS: *zeolite, hierarchical structure, zeolite-structure-directing surfactant, and pseudomorphic crystallization*

INTRODUCTION

Zeolites are a family of crystalline microporous aluminosilicate materials (micropores are defined as pores with diameters <2 nm).[1,2] The unique microporous structure, directed by the structure-directing agent (SDA) such as alkali metal cations and ammoniums (sometimes amines), enables zeolites to have size/shape selective heterogeneous catalytic function.[3−5] Zeolites account for more than 40% of the solid catalytic materials used in the current chemical industry.[6] But, the microporous nature of the zeolites imposes diffusion limitations for bulky molecules.[7−12] Mesoporous aluminosilicate materials with various structures have been synthesized since the 1990s following the synthesis of MCM-41 using surfactant micelles as SDAs (mesopores are defined as 2−50 nm).[13,14] However, such mesoporous materials as composed of amorphous frameworks have insufficient acidity for most petrochemical reactions.[15,16] In recent years, tremendous effort has been put forth to develop synthesis strategies for mesoporous materials that are built with crystalline zeolitic micropore walls.[8,17−25]

Ryoo et al. reported the synthesis of hierarchically microporous/mesoporous zeolites by using an organic surfactant equipped with a multiammonium headgroup.[10,26−32] The multiammonium headgroup can direct crystalline microporous zeolites, while the numerous surfactant molecules are assembled into a micelle that can direct various mesoporous structures depending on the surfactant structure and synthesis condition. The first example of such a hierarchical (or dual) structure-directing surfactant was $[C_{22}H_{45}\text{-}N^+(CH_3)_2\text{-}C_6H_{12}\text{-}N^+(CH_3)_2\text{-}C_6H_{13}][Br]_2$.[10] This surfactant generated MFI zeolite nanosheets with a single-unit-cell thickness of 2.5 nm.[30,31] Later, the dually structure-directing strategy was extended to various zeolites, including a beta zeolite nanosponge, an MFI zeolite nanosponge, and an MFI-like zeolite with hexagonally ordered mesopores.[29,32]

It would be interesting to impart a macropore-generating function into the surfactant molecule so that the molecule can have hierarchically pore-generating functions over the entire scale length, covering macropores (defined as pores with diameters greater than 50 nm), mesopores, and micropores. This challenging problem has not yet been completely resolved. Macropores are too large to inscribe a pore-generating function within a molecule of an ordinary size, even if a self-assembly of molecules is employed. Nevertheless, we point out that it would be possible to generate macropores on top of the mesopore-micropore hierarchy if we can incorporate a pseudomorphic transformation of macroporous silica sources into zeolites. The pseudomorphism involves a phase transformation of the crystal structure or composition without changes in the external form of the original phase.[33] Hence, if the crystallization of zeolite can be controlled in a pseudomorphic manner, then pores greater than 30 nm should be retained from the initial synthesis gel or the zeolite precursor.

In this regard, we tested various surfactants, silica sources, and Na^+ content to synthesize hierarchical beta zeolites. The

Received: March 16, 2012
Revised: June 21, 2012
Published: June 25, 2012

   dx.doi.org/10.1021/cm300841v | *Chem. Mater.* 2012, 24, 2733−2738

zeolite structure and porosity were analyzed by means of X-ray diffraction, N_2 adsorption, and electron microscopy. The result showed, indeed, that the degree of pore retainment could be systematically controlled by the choice of the silica source, surfactant, and Na^+ concentration. We present this zeolite synthesis because this result may provide valuable chemistry for generating a macropore-mesopore-micropore hierarchy in porous materials that might be demanding in some applications handling bulky biogenic substances such as lipids, proteins, and nucleic acids.

EXPERIMENTAL SECTION

Surfactants with β Zeolite-Structure-Directing Groups. Six surfactants were synthesized. Four of them were double-tailed with $-C_{22}H_{45}$ or $-C_{16}H_{33}$ alkyl chains, and the others were single-tailed with $-C_{22}H_{45}$ alkyl chain. The molecular formulas of the double-tailed surfactants are as follows: $[C_{22}H_{45}\text{-}N^+(CH_3)_2\text{-}C_6H_{12}\text{-}N^+(CH_3)_2\text{-}CH_2\text{-}(p\text{-}C_6H_4)\text{-}CH_2\text{-}N^+(CH_3)_2\text{-}C_6H_{12}\text{-}N^+(CH_3)_2\text{-}C_{22}H_{45}][Br^-]_2[Cl^-]_2$, $[C_{22}H_{45}\text{-}N^+(CH_3)_2\text{-}C_6H_{12}\text{-}N^+(CH_3)_2\text{-}CH_2\text{-}(p\text{-}C_6H_4)\text{-}CH_2\text{-}N^+(CH_3)_2\text{-}C_6H_{12}\text{-}N^+(CH_3)_2\text{-}(p\text{-}C_6H_4)\text{-}CH_2\text{-}N^+(CH_3)_2\text{-}C_6H_{12}\text{-}N^+(CH_3)_2\text{-}C_{22}H_{45}][Br^-]_2[Cl^-]_4$, $[C_{22}H_{45}\text{-}N^+(CH_3)_2\text{-}C_6H_{12}\text{-}N^+(CH_3)_2\text{-}CH_2\text{-}(p\text{-}C_6H_4)\text{-}CH_2\text{-}N^+(CH_3)_2\text{-}C_6H_{12}\text{-}N^+(CH_3)_2\text{-}(p\text{-}C_6H_4)\text{-}CH_2\text{-}N^+(CH_3)_2\text{-}C_6H_{12}\text{-}N^+(CH_3)_2\text{-}(p\text{-}C_6H_4)\text{-}CH_2\text{-}N^+(CH_3)_2\text{-}C_6H_{12}\text{-}N^+(CH_3)_2\text{-}C_{22}H_{45}][Br^-]_2[Cl^-]_6$, and $[C_{16}H_{33}\text{-}N^+(CH_3)_2\text{-}C_6H_{12}\text{-}N^+(CH_3)_2\text{-}CH_2\text{-}(p\text{-}C_6H_4)\text{-}CH_2\text{-}N^+(CH_3)_2\text{-}C_6H_{12}\text{-}N^+(CH_3)_2\text{-}(p\text{-}C_6H_4)\text{-}CH_2\text{-}N^+(CH_3)_2\text{-}C_6H_{12}\text{-}N^+(CH_3)_2\text{-}C_{16}H_{33}][Br^-]_2[Cl^-]_4$. These surfactants are denoted as "C_{22}-N_4-C_{22}", "C_{22}-N_6-C_{22}", "C_{22}-N_8-C_{22}", and "C_{16}-N_6-C_{16}" for brevity. In each surfactant, the subscript after "N" indicates the total number of nitrogen atoms in a molecule. The double-tailed surfactants were synthesized as reported elsewhere.[29] The single-tailed surfactants were $[C_{22}H_{45}\text{-}N^+(CH_3)_2\text{-}C_6H_{12}\text{-}N^+(CH_3)_2\text{-}CH_2\text{-}(p\text{-}C_6H_4)\text{-}CH_2\text{-}N^+(CH_3)_2\text{-}C_6H_{12}\text{-}N^+(CH_3)_2\text{-}(p\text{-}C_6H_4)\text{-}CH_2\text{-}N^+(CH_3)_2\text{-}C_6H_{12}\text{-}N^+(CH_3)_2\text{-}C_4H_9][Br^-]_2[Cl^-]_4$ and $[C_{22}H_{45}\text{-}N^+(CH_3)_2\text{-}C_6H_{12}\text{-}N^+(CH_3)_2\text{-}CH_2\text{-}(p\text{-}C_6H_4)\text{-}CH_2\text{-}N^+(CH_3)_2\text{-}C_4H_9][Br^-][Cl^-]_2$. They are denoted as "$C_{22}$-$N_6$-$C_4$" and "$C_{22}$-$N_3$-$C_4$". Their synthesis procedures were similar to the cases of the double-tailed surfactants.

Zeolite Synthesis. *Synthesis of Zeolite β with Diatomaceous Earth.* Zeolite β was hydrothermally synthesized with one of the six surfactants described above. Diatomaceous earth was purchased from Sigma-Aldrich (Hyflo Super Cel). It was used with sodium silicate water glass (Na/Si = 1.75, Shinheung) as a mixed silica source at a ratio of 85: 15. In a typical synthesis experiment, 8.41 g of the sodium silicate solution (diluted to 1.3 wt % SiO_2) was quickly added to an aqueous solution which contained 0.32 g of NaOH, 0.03 g of $Al_2(SO_4)_3$, and a suitable amount of surfactant (1.21 g of C_{22}-N_4-C_{22}, 1.02 g of C_{22}-N_6-C_{22}, 0.92 g of C_{22}-N_8-C_{22}, 0.91 g of C_{16}-N_6-C_{16}, 0.86 g of C_{22}-N_6-C_4, or 0.82 g of C_{22}-N_3-C_4) under magnetic stirring. After stirring for about 5 min, this mixture had 0.54 g of diatomaceous earth added to it. The mixture was shaken by hand for 5 min and then heated in a Teflon-lined autoclave in an oven at 413 K while tumbling. The resultant gel had a molar composition of 1.02 Al_2O_3/ 49.2 SiO_2/ 23 Na_2O/ (20÷n) surfactant/0.66 H_2SO_4/ 5350 H_2O, including the Al source coming from the diatomaceous earth. Here, "n" is the number of N atoms in a surfactant molecule. Sampling was carried out after a desired period of hydrothermal reaction. The precipitated silicates were collected by filtration and dried at 373 K before further analyses were carried out. Samples for the pore-size analysis were calcined in air at 853 K to remove the organic surfactants.

Synthesis of Zeolite β with Tetraethoxysilane (TEOS). The synthesis of zeolite β from TEOS was performed only with C_{22}-N_4-C_{22} under a sodium-free condition. Aluminum isopropoxide (Sigma-Aldrich) was used as an alumina source. The C_{22}-N_4-C_{22} surfactant was used after replacing the halide counterions with OH^- using an anion-exchange resin (MTO−Dowex SBR LCNG OH form, Supelco).[10] In a typical synthesis, TEOS was added to an aqueous solution containing the hydroxide form of C_{22}-N_4-C_{22} and aluminum isopropoxide. The mixture was then vigorously shaken for 30 min. The molar composition of the resultant gel was 30 SiO_2/ 1 Al_2O_3/ 1.4 C_{22}-N_4-C_{22} (hydroxide form)/ 1000 H_2O/120 ethanol. This gel was heated for 6 d in an oven at 413 K while tumbling. The zeolite product was collected by filtration. After drying at 373 K, the product was calcined in air at 853 K to remove the organic surfactant.

To investigate the effect of Na^+, the zeolite β was synthesized under the same conditions above except with sodium aluminate (53 wt % of Al_2O_3 and 42.5 wt % of Na_2O) as the Al source instead of aluminum isopropoxide. In this case, the initial gel composition was 30 SiO_2/ 1 Al_2O_3/ 1.32 Na_2O/1.4 C_{22}-N_4-C_{22} (hydroxide-form)/ 1000 H_2O/120 ethanol.

Characterization of Zeolite Products. X-ray diffraction (XRD) patterns were taken with a Rigaku Multiflex diffractometer equipped with CuKα radiation (40 kV, 40 mA). Transmission electron micrograph (TEM) images were obtained by a Philips F30 Tecnai at an operating voltage of 300 kV. The N_2 adsorption isotherms were measured at the liquid nitrogen temperature with an ASAP 2020 volumetric adsorption analyzer. Scanning electron micrograph (SEM) images were obtained without a metal coating, operating either a Hitachi S-4800 at 2 kV or a JEOL JSM-7401F instrument at 0.8−1.0 kV (retarding bias: 0.2 kV). For the SEM investigation of the internal structure, the solid precipitates were sampled at several reaction times during the zeolite synthesis process with C_{22}-N_8-C_{22}. The samples were cross-section polished for 6 h by JEOL SM-09010 using accelerated argon ions (6 kV, 120 mA).[34,35]

RESULTS AND DISCUSSION

Transformation of Diatomaceous Earth into Zeolite β. Figure 1A shows XRD patterns of solid-state residues collected

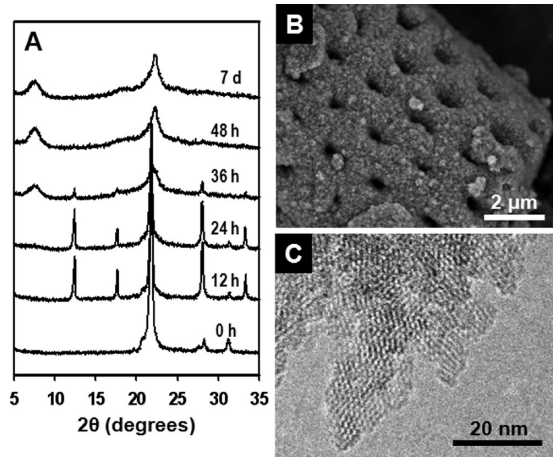

Figure 1. (A) XRD patterns of as-synthesized solid precipitates collected after various hydrothermal synthesis times (0 h−7 d). The synthesis was performed with using diatomaceous earth as a silica source and a zeolite structure-directing surfactant denoted as C_{22}-N_8-C_{22} at 413 K from the molar composition of 1.02 Al_2O_3/ 49.2 SiO_2/ 23 Na_2O/2.5 C_{22}-N_8-C_{22}/ 0.66 H_2SO_4/ 5350 H_2O. (B) SEM and (C) TEM images of the final zeolite β product collected at 48 h.

from the hydrothermal reaction mixture at various reaction times after starting with diatomaceous earth as a zeolite precursor with the C_{22}-N_8-C_{22} surfactant. The XRD profile of the initial gel (0 h) shows the typical XRD pattern of diatomaceous earth. The XRD pattern shows three sharp peaks at 22, 28, and 31° of the 2θ values. These XRD peaks are assigned to the Bragg diffraction coming from the crystal structure of the cristobalite phase, which is often present as a minor component in the amorphous silica of diatomaceous earths. The intensity of the diffraction decreased to approximately 60% in 12 h of the hydrothermal reaction. In this case, however, four sharp peaks appeared at 12, 17.5, 26,

dx.doi.org/10.1021/cm300841v | Chem. Mater. 2012, 24, 2733−2738

and 33°. These new peaks were attributed to the formation of zeolite P. Both the zeolite P and the cristobalite phases disappeared almost completely at 36 h. At the same time, new broad peaks appeared at 7.5, 17.5, and 22° of 2θ. At 48 h, other peaks disappeared completely. The new XRD pattern indicates the formation of a hierarchical zeolite β, a contention which is based on our earlier work using zeolite structure-directing surfactants and sodium silicate. Figure 1B shows a representative SEM image of the zeolite product collected at 48 h. The overall image retained the shape of the diatom fossils used in the silica source. Upon high magnification, however, the detailed surfaces show roughness due to the formation of tiny nanoparticles. Figure 1C shows a representative TEM image of the zeolite product. This TEM image revealed that the product was indeed a zeolite β nanosponge. The framework of the zeolite nanosponge was loosely assembled in a disordered manner, possessing a high specific volume of mesopores.

Figure 2 shows a N_2 sorption isotherm obtained from the 48-h sample at 77 K, with its corresponding pore size distributions.

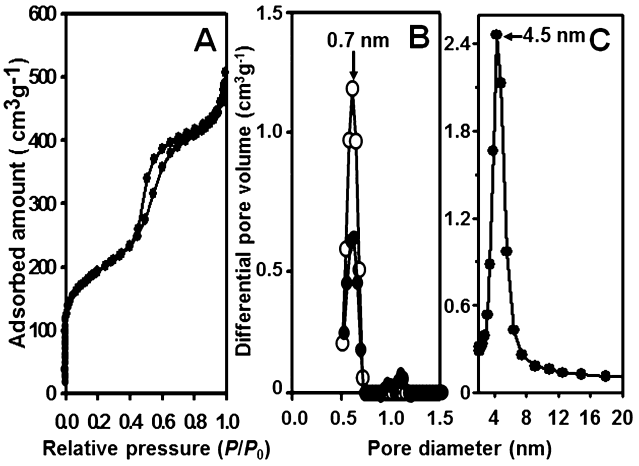

Figure 2. (A) N_2 sorption isotherm of the zeolite β synthesized using diatomaceous earth and C_{22}-N_8-C_{22}, (B) corresponding micropore size distribution derived by a NLDFT analysis, and (C) mesopore size distribution obtained from an adsorption branch using the BJH algorithm. For comparison, the micropore size distribution of conventional zeolite β is included in (B) as the open circles.

The adsorption isotherm exhibits a very sharp increase in the low-pressure region of $P/P_0 < 0.1$ and another jump in the medium-pressure region of $0.4 < P/P_0 < 0.5$. The former could be interpreted as due to the N_2 filling in the micropores, and the latter to capillary condensation in the mesopores. The micropore diameters were determined from the adsorption isotherm in the region of $P/P_0 < 0.1$ according to the nonlocal density functional theory (NLDFT).[36] The result showed a very sharp distribution peak centered at 0.70 nm, which was consistent with micropores in zeolite β. On the other hand, the mesopore diameters were determined from the adsorption branch in the region of $0.4 < P/P_0 < 0.5$. The Barrett–Joyner–Halenda (BJH) algorithm was used for the mesopore analysis. The mesopore-size distribution obtained in this manner showed a narrow peak center at 4.5 nm.

The presence of the micropores and mesopores is in good agreement with the hierarchically nanoporous structure of the zeolite β framework, which can be inferred from the TEM image in Figure 1C. In this nanosponge, the mesopores are present between the nearest neighboring frameworks. The mesopore diameters are quite uniform, despite the irregular arrangements of the frameworks, reflecting that the surfactant micelles are mesopore templates. On the other hand, the microporous frameworks are generated by the SDA ammonium groups in the surfactants.[29] Normally, zeolitic frameworks generated by such surfactant-type SDAs are highly uniform in thickness. The framework thickness can be determined by a N_2 adsorption isotherm of its carbon replica.[29,37] The framework thickness of the present zeolite measured in this manner is 5.1 nm. This result confirms that the mesopores and micropores could be generated because of the dual structure-directing role of the surfactant. A similarly hierarchical zeolite was synthesized using sodium silicate water glass in a previous study by the authors.[29] A notable difference from the previous work is that the present β zeolite exhibits a diatom fossil-like macroporous morphology (macropore diameters $\approx$ 0.3 μm). The macropores must be retained from the zeolite precursor. These macropores form an additional level of large pores on top of the mesopore-micropore hierarchy. In total, the present zeolite β has three levels of pores (macropore-mesopore-micropore) that are structured hierarchically.

The zeolite formation process was investigated in more detail with high-resolution SEM in combination with the XRD patterns in Figure 1A. The SEM images are shown in Figure 3.

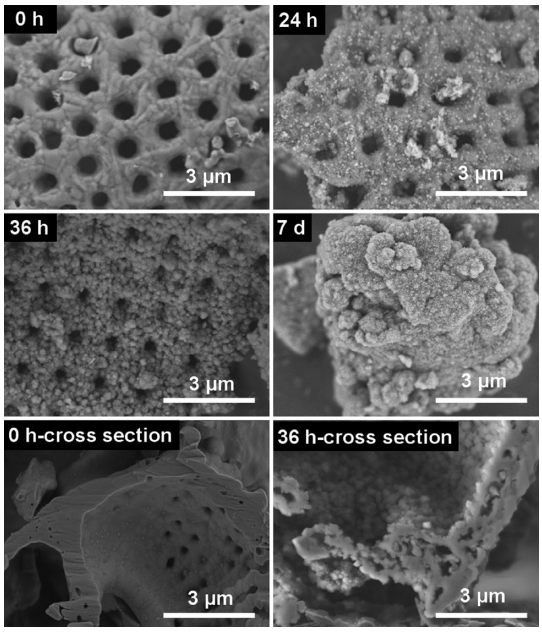

Figure 3. High-resolution SEM images of as-synthesized solid precipitates collected from the synthesis mixture at various hydrothermal synthesis times using the C_{22}-N_8-C_{22} surfactant. The four upper images show the change of external morphology during the crystallization of diatomaceous earth into zeolite β. The two bottom images are cross-sectional views of 0 and 36 h samples polished by an argon ion beam.

The sample at 0 h in Figure 3 was collected after filtration of the initial synthesis gel just before it was heated to 413 K. Other samples were collected at various times in the middle of the hydrothermal reaction at 413 K. The morphology of the 0-h sample is very similar to the diatomaceous earth used as the zeolite precursor, except for the slightly rugged surfaces. The surface roughness was likely due to partial dissolution or swelling under the basic condition in the gel state. After 24 h of

dx.doi.org/10.1021/cm300841v | Chem. Mater. 2012, 24, 2733–2738

hydrothermal reaction at 413 K, the sample still retained the overall morphology of the diatomaceous earth. The detailed surfaces became more rugged, and tiny particles adhered to them (6 nm in diameter; shown as the bright spots in the SEM image). These particles were confirmed as crystallites of zeolite β in the TEM investigation. The crystallites showed lattice fringes with a d-spacing of 1.22 nm. This spacing corresponds to d_{100} of zeolite β. At this time of reaction, bulk crystals about 3 μm in diameter were occasionally observed in the SEM images. The crystal morphologies were completely different from the diatomaceous earth particles. These crystals were confirmed as a zeolite P phase by TEM and electron diffraction patterns. The zeolite P particles are believed to form through a solution-mediated route from dissolved silicates and aluminates in the synthetic composition. During such an early period of hydrothermal reaction, the diatomaceous earth would remain without significant dissolution into the solution. As a result, the concentration of the silicate is believed to be temporarily low, thus becoming favorable for the formation of zeolite P.[1,2] The zeolite P phase disappeared completely as the reaction time increased to 48 h. The entire sample became a high-purity zeolite β, as determined by XRD and TEM. The conversion of zeolite P to β by the C_{22}-N_8-C_{22} surfactant was similar to other SDA-mediated conversion of P to high-silica zeolites.[38,39]

Except for the detailed roughness of surfaces, the overall morphology of the zeolite precursor (i.e., diatomaceous earth) was well retained when the zeolite β formation was just completed (in 48 h). The retainment of the original morphology can be explained by a pseudomorphic transformation in which the solid-state silica source transforms into crystalline zeolite without migrating away into the solution phase.[40] However, the diatom-like morphology was lost in 7 d under the reaction condition. This result indicates that the zeolite product continued to change morphologies through a dissolution-recrystallization process, which is similar to Ostwald ripening. In this manner, the initial zeolite formation can be regarded as a type of pseudomorphism, but over the long-term, the process is not perfectly pseudomorphic. Nonetheless, the recrystallization process can be sufficiently slow such that the zeolite product with the morphologies of diatomaceous earth can be collected even under a high Na^+ concentration (Na^+/Si = 1).

To investigate the internal morphology, the samples collected at 0 and 36 h were examined by a high-resolution SEM microscope after being cross-sectioned with an Ar ion beam.[34,35] The two SEM images in the bottom of Figure 3 were taken on the cross-sectioned surfaces of the two samples. The internal part of the 0-h sample was almost completely filled with the silicate solids. In contrast, the 36-h sample showed many cavities. The formation of cavities indicates that the internal part of the diatomaceous earth is dissolved and supplied for zeolite crystallization in the outside rims.

Effects of Surfactant Structures for Pseudomorphic Transformation. From the comparison of the SEM image shown in Figure 1B with those in Figure 4, it is notable that the faithfulness to the pseudomorphic generation of zeolite β becomes progressively improved in the order of C_{22}-N_4-C_{22} < C_{22}-N_6-C_{22} < C_{22}-N_8-C_{22}. A similar comparison can be done in the case of C_{22}-N_3-C_4 < C_{22}-N_6-C_4. These pseudomorphic trends may be correlated to the number of ammonium groups in the surfactant. As for ordinary SDAs, it was already reported that multiammoniums are superior to monoammoniums for the pseudomorphic generation of zeolites.[41−43] The behavior of the

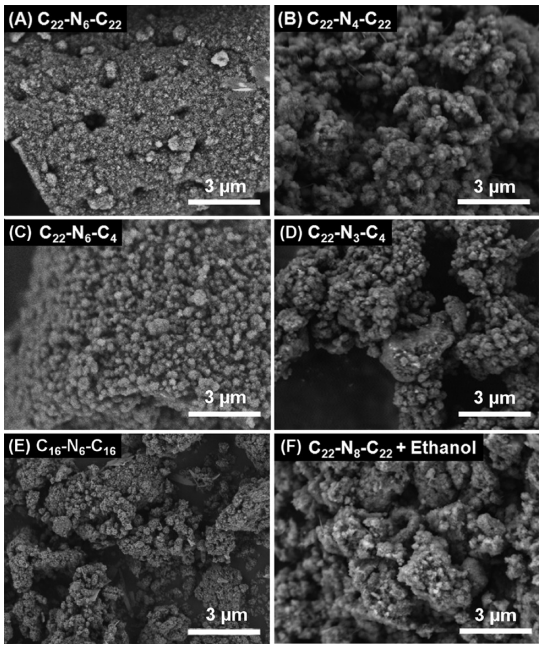

Figure 4. SEM images of zeolite β products crystallized from diatomaceous earth while varying the surfactant type: (A) C_{22}-N_6-C_{22}, (B) C_{22}-N_4-C_{22}, (C) C_{22}-N_6-C_4, (D) C_{22}-N_3-C_4, (E) C_{16}-N_6-C_{16}, and (F) C_{22}-N_8-C_{22}. The synthesis was performed in the gel composition of 1.02 Al_2O_3/ 49.2 SiO_2/ 23 Na_2O/ ((20÷n) surfactant/0.66 H_2SO_4/ 5350 H_2O/ m ethanol. "n" corresponds to the number of nitrogen molecules in each surfactant. "m" is 0 for (A−E) or 250 for (F).

multiammonium SDAs was attributed to their multiple binding to silica sources, which might lead to the formation of highly stable silicate gel that would not be easily soluble into the solution phase.[44,45] In the case of C_{22}-N_6-C_{22} and C_{22}-N_6-C_4, the two surfactants have the same number of ammoniums. Nevertheless, the double-tailed surfactant is better for the pseudomorphic zeolite generation. Similarly, when C_{22}-N_6-C_{22} and C_{16}-N_6-C_{16} are compared, the surfactant with longer tails is better. This result suggests that a surfactant with stronger hydrophobic interactions between tails would be more favorable for the pseudomorphic zeolite generation. Such a surfactant would agglomerate into micelles more readily, and the co-operative binding of many ammonium groups seems to cause a similar effect to the aforementioned multiple binding effects. To check the micellization effect, we added ethanol to the synthesis mixture containing the C_{22}-N_8-C_{22} surfactant. The resultant zeolite samples showed that the pseudomorphism became less faithful as the amount of ethanol was increased (comparing Figure 1B and Figure 4F). Ethanol is well-known to increase the solubility of organic surfactants in an aqueous solution and thereby to inhibit the micellization of the surfactant molecules.

The pseudomorphic generation of the zeolite depends on many other synthesis factors such as the silica source, hydrothermal reaction temperature, Na^+ concentration, and pH, in addition to the SDA. However, even in our best obtainable result using diatomaceous earth and C_{22}-N_8-C_{22}, it is not a perfect pseudomorphism at all. The transformation of the silica source appears to be pseudomorphic only at the macrosize scale.[1,46] Cracks and pores can be generated in the detailed internal structure and at the surfaces for various reasons such as a change in the density and the tendency of the

dx.doi.org/10.1021/cm300841v | Chem. Mater. 2012, 24, 2733−2738

crystal to grow with a specific orientation. At the nanoscale, this process can result in a total change of morphology.

Faithful Retainment of Nanopores in a Synthesis Gel. The above findings are applicable to the pseudomorphic retainment of nanopores that are formed initially during the preparation of zeolite synthesis gel. As mentioned above, our zeolite products can change the morphology through dissolution-recrystallization processes. In principle, these processes can be retarded by removing Na^+ from the synthetic composition.[10,26] However, the Na^+-free synthesis is not practically feasible in the present synthesis of the zeolite β using diatomaceous earth at 413 K, as the zeolite formation occurs too slowly without Na^+ at 413 K. However, the temperature cannot be increased further as the structure-directing surfactant is decomposed. A detour to investigate the effect of the Na^+-free synthesis condition is to use TEOS instead of diatomaceous earth. TEOS is a much more reactive silica source than diatomaceous earth, which can generate zeolite β at 413 K even without Na^+. Therefore, we synthesized two samples of zeolite β using TEOS and C_{22}-N_4-C_{22} at 413 K. One sample was synthesized under a Na^+-free condition. The other was obtained in the presence of Na^+ (Na^+/Si = 0.088, as described in the Experimental Section). In both cases, the resultant products were crystalline zeolite β. Both zeolites had a very fluffy and highly porous texture, as shown in Figure 5A. However, they exhibited a notable difference in the distribution of their mesopores (see Figures 5B and 5C).

Figures 5B and 5C show their difference in the mesopore size distribution. In the case of the Na^+-free synthesis, the zeolite β shows two distinct mesopore peaks, one centered at 3.7 and the other at 30 nm. Thus, the zeolite sample has a hierarchy of three different pore levels, including the intrinsic 0.7-nm micropores of the zeolite (the micropore size distribution is not shown in Figure 5B). Among the two types of mesopores, the 3.7-nm peak can be assigned to the mesopores generated owing to the templating effect of the C_{22}-N_4-C_{22} surfactant micelles. On the other hand, the 30-nm peak can be assigned to the large mesopores corresponding to the gel pores which were present in the initial synthetic gel. This assignment is supported by the fact that the synthetic gel also exhibits a mesopore peak that is very similar to the 30-nm peak. On the basis of this result, we believe that the pseudomorphic zeolite generation can occur so faithfully as to retain the 30-nm gel pores. When Na^+ was present (Na^+/Si = 0.088), however, the zeolite synthesis failed to retain the gel pores. The resultant pore size distribution curves show that the initial gel pores disappeared in the final zeolite product (see Figure 5C). A similar result was obtained when the Na^+/Si ratio was adjusted by the addition of NaCl instead of Na_2O. This result indicates that the disappearance of the gel pores was not due to the pH increase caused by the addition of a sodium hydroxide. In fact, Na^+ ions are known to have catalytic activities for increasing the rates of both silicate polymerization and hydrolysis at the same time.[1] The Na^+ ions appeared to cause the gel pores to disappear, through a catalytic transformation that could make the local structure more condensed.

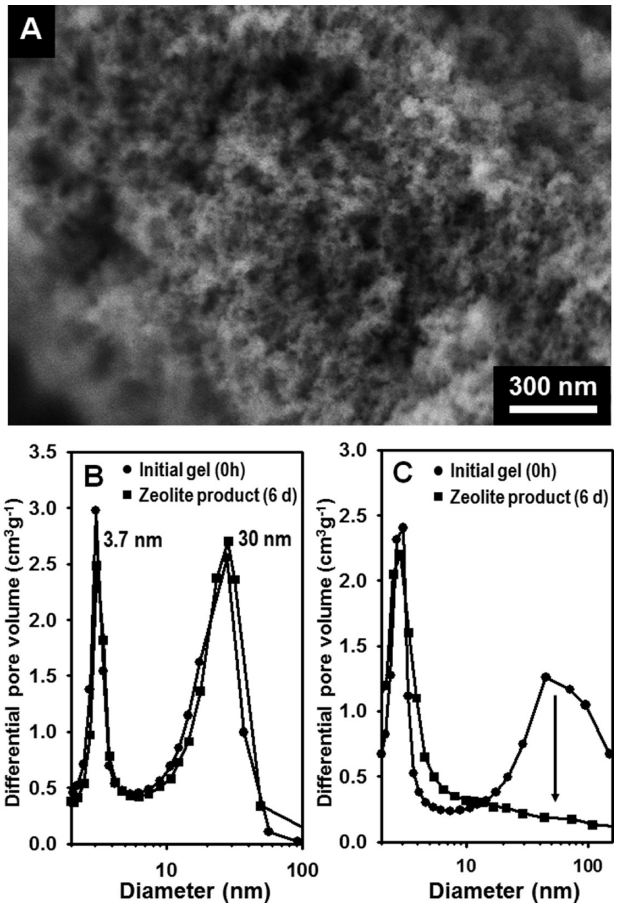

Figure 5. (A) SEM image of zeolite β collected after a hydrothermal time of 6 d with the synthesis gel containing the C_{22}-N_4-C_{22} surfactant and tetraethoxysilane (TEOS) under the Na^+-free condition, and (B) its mesopore size distribution in comparison with that of the initial gel (0 h). For further comparison, a change in the mesopore size distribution of the initial gel (0 h) and the zeolite β product (6 d) obtained from the synthesis gel containing Na^+ (Na^+/Si = 0.088) is shown in (C).

CONCLUSION

Various types of organic surfactants could be synthesized by bonding a zeolite-structure-directing group (a multiammonium ion or other suitable one) into one or more hydrophobic tails. These surfactants could function as structure-directing agents for the hydrothermal synthesis of zeolites, exhibiting a mesopore-micropore hierarchy. In this manner, two pore-generating functions (i.e., microporogenic and mesoporogenic) were inscribed within a surfactant molecule. Our further challenge was to add a macropore-generating function to the surfactant. However, the macropores remained too large to be generated by a molecular porogenic function. Instead, such macropores could be generated by retaining pores from the initial synthesis gel or a porous precursor via a pseudomorphic transformation route. These pores became more faithfully retained as the Na^+ concentration decreased in the synthesis composition, as the hydrophobic interactions increased between the surfactant molecules, and as the number of ammoniums increased in the surfactant molecules. This synthesis principle has been demonstrated for zeolite β, but we believe that it would be further extended to other zeolites. Zeolite with a macropore-mesopore-micropore hierarchy might be useful where it is necessary to accommodate bulky biogenic substances such as lipids, proteins, and nucleic acids, in addition to the ion-exchange capacity of the zeolite frameworks.

AUTHOR INFORMATION

Corresponding Author
*E-mail: rryoo@kaist.ac.kr.

Notes

The authors declare no competing financial interest.

■ ACKNOWLEDGMENTS

This work was supported by the National Honor Scientist Program (20110031411) and by the World Class University Program (R31-2011-000-10071-0) of the Ministry of Education, Science and Technology in Korea.

■ REFERENCES

(1) Breck, D. W. *Zeolite Molecular Sieves*; Wiley and Sons: New York, 1974.
(2) http://www.iza-online.org/ (International Zeolite Association Home Page).
(3) Cundy, C. S.; Cox, P. A. *Chem. Rev.* **2003**, *103*, 663.
(4) Corma, A. *Chem. Rev.* **1997**, *97*, 2373.
(5) Davis, M. E. *Nature* **2002**, *417*, 813.
(6) Tanabe, K.; Hölderich, W. F. *Appl. Catal. A: Gen.* **1999**, *181*, 399.
(7) Corma, A. *J. Catal.* **2003**, *216*, 298.
(8) Choi, M.; Cho, H. S.; Srivastava, R.; Venkatesan, C.; Choi, D.-H.; Ryoo, R. *Nat. Mater.* **2006**, *5*, 718.
(9) Srivastava, R.; Choi, M.; Ryoo, R. *Chem. Commun.* **2006**, 4489.
(10) Choi, M.; Na, K.; Kim, J.; Sakamoto, Y.; Terasaki, O.; Ryoo, R. *Nature* **2009**, *461*, 246.
(11) Kim, J.; Choi, M.; Ryoo, R. *J. Catal.* **2010**, *269*, 219.
(12) Kim, J.; Park, W.; Ryoo, R. *ACS Catal.* **2011**, *1*, 337.
(13) Kresge, C. T.; Leonowicz, M. E.; Roth, W. J.; Vartuli, J. C.; Beck, J. S. *Nature* **1992**, *359*, 710.
(14) Beck, J. S.; Vartuli, J. C.; Roth, W. J.; Leonowicz, M. E.; Kresge, C. T.; Schmitt, K. D.; Chu, C. T. W.; Olson, D. H.; Sheppard, E. W.; McCullen, S. B.; Higgins, J. B.; Schlenker, J. L. *J. Am. Chem. Soc.* **1992**, *114*, 10834.
(15) Cassiers, K.; Linssen, T.; Mathieu, M.; Benjelloun, M.; Schrijnemakers, K.; Van Der Voort, P.; Vansant, E. F. *Chem. Mater.* **2002**, *14*, 2317.
(16) Zhao, D.; Nie, C.; Zhou, Y.; Xia, S.; Huang, L.; Li, Q. *Catal. Today* **2001**, *68*, 11.
(17) Beck, J. S.; Vartulli, J. C.; Kennedy, G. J.; Kresge, C. T.; Roth, W. J.; Schramm, S. E. *Chem. Mater.* **1994**, *6*, 1816.
(18) Karlsson, A.; Stocker, M.; Schmidt, R. *Microporous Mesoporous Mater.* **1999**, *27*, 181.
(19) Petkov, N.; Holzl, M.; Metzger, T. H.; Mintova, S.; Bein, T. *J. Phys. Chem. B* **2005**, *109*, 4485.
(20) Liu, Y.; Zhang, W. Z.; Pinnavaia, T. J. *J. Am. Chem. Soc.* **2000**, *122*, 8791.
(21) Zhang, Z.; Han, Y.; Xiao, F.-S.; Qiu, S.; Zhu, L.; Wang, R.; Yu, Y.; Zhang, Z.; Zou, B.; Wang, Y.; Sun, H.; Zhao, D.; Wei, Y. *J. Am. Chem. Soc.* **2001**, *123*, 5014.
(22) Choi, M.; Srivastava, R.; Ryoo, R. *Chem. Commun.* **2006**, 4380.
(23) Cho, K.; Cho, H. S.; de Menorval, L.-C.; Ryoo, R. *Chem. Mater.* **2009**, *21*, 5664.
(24) Choi, M.; Lee, D.-H.; Na, K.; Yu, B.-W.; Ryoo, R. *Angew. Chem., Int. Ed.* **2009**, *48*, 3673.
(25) Valiullin, R.; Kärger, J.; Cho, K.; Choi, M.; Ryoo, R. *Microporous Mesoporous Mater.* **2011**, *142*, 236.
(26) Na, K.; Choi, M.; Park, W.; Sakamoto, Y.; Terasaki, O.; Ryoo, R. *J. Am. Chem. Soc.* **2010**, *132*, 4169.
(27) Na, K.; Park, W.; Seo, Y.; Ryoo, R. *Chem. Mater.* **2011**, *23*, 1273.
(28) Na, K.; Jo, C.; Kim, J.; Ahn, W.-S.; Ryoo, R. *ACS Catal.* **2011**, *3*, 1435.
(29) Na, K.; Jo, C.; Kim, J.; Cho, K.; Jung, J.; Seo, Y.; Messinger, R. J.; Chmelka, B. F.; Ryoo, R. *Science* **2011**, *333*, 328.
(30) Park, W.; Yu, D.; Na, K.; Jelfs, K. E.; Slater, B.; Sakamoto, Y.; Ryoo, R. *Chem. Mater.* **2011**, *23*, 5131.
(31) Jung, J.; Jo, C.; Cho, K.; Ryoo, R. *J. Mater. Chem.* **2011**, *22*, 4637.
(32) Na, K.; Choi, M.; Ryoo, R. *Microporous Mesoporous Mater.* **2012**, in press (DOI:10.1016/j.micromeso.2012.03.054).
(33) Baur, W. H. *Microporous Mesoporous Mater.* **1998**, *25*, 229.
(34) Stevens, S. M.; Jansson, K.; Xiao, C.; Asahina, S.; Klingstedt, M.; Grüner, D.; Sakamoto, Y.; Miyasaka, K.; Cubillas, P.; Brent, R.; Han, L.; Che, S.; Ryoo, R.; Zhao, D.; Anderson, M. W.; Schüth, F.; Terasaki, O. *JEOL News* **2009**, *44*, 17.
(35) Cho, K.; Ryoo, R.; Asahina, S.; Xiao, C.; Klingstedt, M.; Umemura, A.; Anderson, M. W.; Terasaki, O. *Solid State Sci.* **2011**, *13*, 750.
(36) Ravikovitch, P. I.; Domhnaill, S. C. O.; Neimark, A. V.; Schueth, F.; Unger, K. K. *Langmuir* **1995**, *11*, 4765.
(37) Ryoo, R.; Joo, S. H.; Jun, S. *J. Phys. Chem. B* **1999**, *103*, 7743.
(38) Zones, S. I. *J. Chem. Soc., Faraday Trans.* **1990**, *86*, 3467.
(39) Zones, S. I.; Van Nordstrand, R. A. *Zeolites* **1988**, *8*, 166.
(40) Cundy, C. S.; Cox, P. A. *Microporous Mesoporous Mater.* **2005**, *82*, 1.
(41) Beck, L. W.; Davis, M. E. *Microporous Mesoporous Mater.* **1998**, *22*, 107.
(42) Lai, Z.; Bonilla, G.; Diaz, I.; Nery, J. G.; Sujaoti, K.; Amat, M. A.; Kokkoli, E.; Terasaki, O.; Thompson, R. W.; Tsapatsis, M.; Vlachos, D. G. *Science* **2001**, *18*, 456.
(43) Bonilla, G.; Diaz, I.; Tsapatsis, M.; Jeong, H.-K.; Lee, Y.; Vlachos, D. G. *Chem. Mater.* **2004**, *16*, 5697.
(44) Choi, M.; Na, K.; Ryoo, R. *Chem. Commun.* **2009**, 2845.
(45) Na, K.; Choi, M.; Ryoo, R. *J. Mater. Chem.* **2009**, *19*, 6713.
(46) Lee, Y. J.; Lee, J. S.; Park, Y. S.; Yoon, K. B. *Adv. Mater.* **2001**, *13*, 1259.